A Letters Journal Exploring the Frontiers of Physics

April 2014

EPL, **106** (2014) 27007
doi: 10.1209/0295-5075/106/27007

www.epljournal.org

Velocity autocorrelation spectra in molten polymers measured by NMR modulated gradient spin-echo

Janez Stepišnik[1,2], Aleš Mohorič[1,2], Carlos Mattea[3], Siegfried Stapf[3] and Igor Serša[1,2,4]

[1] *University of Ljubljana, FMF - Jadranska 19, 1000 Ljubljana, Slovenia, EU*
[2] *Institute Jozef Stefan - Jamova 39, 1000 Ljubljana, Slovenia, EU*
[3] *Ilmenau University of Technology - Ilmenau, Germany, EU*
[4] *Department of Biomedical Engineering, Kyung Hee University - Suwon, Korea*

received 6 January 2014; accepted in final form 4 April 2014
published online 22 April 2014

PACS 76.60.Lz – Spin echoes
PACS 36.20.Ey – Macromolecules and polymer molecules: Conformation (statistics and dynamics)
PACS 61.25.H- – Macromolecular and polymers solutions; polymer melts

Abstract – The segmental dynamics in molten linear polymers is studied by the NMR method of modulated gradient spin-echo, which directly probes a spectrum of molecular velocity autocorrelation function. Diffusion spectra of mono-disperse poly(isoprene-1.4) with different molecular masses, measured in the frequency range 0.1–10 kHz at a temperature of 26 °C, have a form similar to the spectrum of Rouse chain dynamics, which implicates the tube-Rouse motion as the dominant dynamic process in this frequency range. The scaling of the center-of-mass diffusion coefficient, given from the fitting parameters, changes from N^{-1} into $N^{-2.4}$ at around $N \approx 3$–5 Kuhn steps, which is less than predicted by theory and simulations, while the correlation times of the tube-Rouse mode do not follow the anticipated scaling.

Introduction. – High density, entanglements, chain-bonds and cross-links hinder the formulation of an explicit theory of molecular dynamics in molten polymers which remains an incompletely understood puzzle. Despite the efforts to solve this problem in recent decades, the theory of polymer dynamics is still based on highly simplified models. Among the most widely known are the Rouse [1] and the tube/reptation models [2,3]. In the later, "the reptation" describes a snake-like creeping of a polymer chain during the Brownian motion along a fictive tube formed by adjacent chains of overlapped polymers. These models neglect the details of a chain structure and are applicable only on the length scales, where a molecule behaves as a highly flexible chain with universal properties. In the Rouse model, a molecule is described as a Gaussian chain of beads connected by springs interacting with a stochastic medium to mimic the presence of other chains. The model predicts the scaling of the chain center-of-mass diffusion coefficient as $N^{-\nu}$ with $\nu = 1$ and N is the number of Kuhn steps. In the tube/reptation model, adjacent chains restrict the motion of a polymer chain in directions normal to its length and force the center-of-weight diffusion coefficient to scale with $\nu = 2$ for chains long enough to entangle, *i.e.* $N > N_e$, where N_e corresponds to the number of Kuhn steps between two entanglements. Improved versions of the reptation theory [4,5] and of the mode coupling theory [6,7] put ν in the range 2–2.25. Molecular dynamics simulations of polymeric ensembles [8–10] show the transition from the Rouse to the reptation regime with $\nu > 1$ for N in the interval 6–90, and with $\nu = 2.4$ for $N > 150$. Generally, there is no clear consensus in the literature on the entanglement length that corresponds to the crossover between the Rouse and tube/reptation regime, nor on the self-diffusion scaling.

All along, there is a concern over the validity of the tube concept in polymer melts, where the tube arises from constraints imposed by surrounding chains. The overall motion of chains releases tube's constraints affecting the motion of tube segments and the lifetime of a tube. A lot of effort has been made to find a suitable approximation for the tube constraint release, however, the problem remains unsolved to these days [11].

Structural and dynamical properties of polymers predicted by models are in qualitative agreement with experimental data resulting from different methods, some of which are no longer limited to a macroscopic, rheological

view, but enable a direct insight into the polymer dynamics on the segmental scale [11]. In polymer melt, the chains exhibit a complex hierarchy of dynamic processes, starting with very fast and local conformational rearrangements on the picoseconds scale, which can be measured by neutron scattering [12], and extending into the range of seconds for slow, diffusive and cooperative motions that can be observed by the methods of nuclear magnetic resonance (NMR). NMR methods provide information about molecular motion, either indirectly by the analysis of spin relaxation data [13–16] or by measuring directly the displacement of spin bearing molecules by the gradient spin-echo (GSE) [14,17]. The fast motion of Rouse modes, hindered by topological restrictions, induces long-lived orientational correlation linked to microscopic parameters observable by the spin relaxation. The relationship between polymer chain dynamics and NMR spin relaxation is caused by the orientational dependence of the dipolar coupling between adjacent spins, which fluctuates rapidly and mirrors the segmental dynamics through the magnetic dipole-dipole correlation function [18,19], which contains the intramolecular and the intermolecular contributions. Intramolecular interactions fluctuate due to molecular rotation, while the intermolecular couplings depend also on the relative translational motion of the molecules, which significantly affects the spin-lattice relaxation measurements at low Larmor frequencies. Thus, the study of polymer dynamics by the NMR spin relaxation requires the disentanglement of reorientational and translational dynamics that is solved by the use of the isotope dilution technique at the field-cycling and transverse NMR relaxometry [14,20], by combining the NMR relaxometry and the dielectric spectroscopy [21,22], or by the double-quantum NMR experiments [15,16,23] etc. Different models and approximations of polymer dynamics have been discussed in the context of different spin relaxation studies, but failing to give an exact form of the correlation function. Although, these experiments generally confirm the scaling laws of the reptation model [19].

Polymer dynamics was studied also by the GSE method, which provides direct information about the displacement of spin bearing particles in the time interval of spin dephasing in the inhomogeneous magnetic field and the subsequent refocusing by means of a radio-frequency pulse. The method is suitable to test model predictions of the segment displacement within the time scales that range from milliseconds up to the order of seconds, *i.e.*, to scales inaccessible by other techniques such as radioactive tracer and quasielastic neutron scattering experiments but which overlap with NMR field cycling relaxometry in the interval of milliseconds. Provided the measuring intervals longer than the terminal relaxation time, which is defined as the terminal or asymptotic viscous decay of the polymer in the rheology, the GSE method can give the polymer center-of-mass diffusion coefficient in the polymer melt. Otherwise, the obtained segmental displacement is not linear in time, and is termed anomalous diffusion [17,24,25]. Anomalous diffusion reflects the segmental motions within the length scale of a random polymer coil and is supposed to be a consequence of a combined effect of flip-flop spin diffusion and segmental diffusion on the basis of the reptation model [26,27]. The GSE measurements of molten polydispersed polymers give the center-of-mass diffusion coefficient that scales with $\nu = 2$ for polymers with $N > N_e$, and as $\nu = 1$ below N_e [24]. However, the subsequent GSE measurements of very mono-dispersed molten polymers [28,29] do not confirm this result, but give $\nu > 2$ scaling for the total range of polymer lengths without any crossover to $\nu = 1$ for short chains. These conflicting results may result either from poorly determining the center-of-mass diffusion coefficient without considering the crossover to the anomalous diffusion regime at the same time [17] or by the fact that a strong internal susceptibility magnetic field at the interstices of voids in the polymer melt might spoil the measurement [14]. Several methods were proposed to minimize the effect of the internal gradient [30–32], but an experimental method that could avoid these problems is beneficial.

Modulated gradient spin-echo. – Such method is the modulated gradient spin-echo (MGSE) [33], which directly probes the low-frequency part of the velocity autocorrelation spectrum (VAS) of spin bearing particles

$$D(\omega) = \int_0^\infty \langle \Delta v_z(t) \Delta v_z(0) \rangle e^{i\omega t} \mathrm{d}t, \qquad (1)$$

where $\Delta v_z(t) = v_z(t) - \langle v_z(t) \rangle$ is the velocity fluctuation in the direction of the magnetic field gradient applied along the z-axis. By using a sequence of radio-frequency (RF) pulses and inhomogeneous magnetic field, *i.e.* the magnetic field gradient, the attenuation of the spin-echo appears as

$$-\ln E(\tau)/E_0 = \beta(\tau) = \frac{1}{\pi} \int_0^\infty |q(\omega, \tau)|^2 D(\omega) \mathrm{d}\omega, \qquad (2)$$

where τ is the time of signal acquisition, $q(\omega, \tau)$ is the spectrum of spin phase discordance by the RF/gradient sequence and E_0 is the magnitude of the spin-echo in the absence of the magnetic-field gradient, $\mathbf{G} = \nabla |\mathbf{B}(\mathbf{r})|$ [34,35]. MGSE is the sequence of RF/gradient pulses, which modulates the spin phases discordance so as to obtain the spectrum $|q(\omega, \tau)|^2$ with a narrow peak at the modulation frequency [36] enabling the sampling of $D(\omega)$ by changing the modulation period. The upper frequency limit of the method is determined by the highest switching rate of the sequence and the lower one by the spin relaxation. In the first MGSE applications [33,36], where a train of π-RF pulses was interspersed by gradient pulses [37–40], the highest achievable frequency was below 1 kHz due to a slew rate limitation of the gradient system. Using the CPMG train of π-RF pulses [41] with a constant gradient [42–44], we avoid the problem of the gradient slew rate and set the upper frequency limit to the duty cycle of the RF amplifier, which

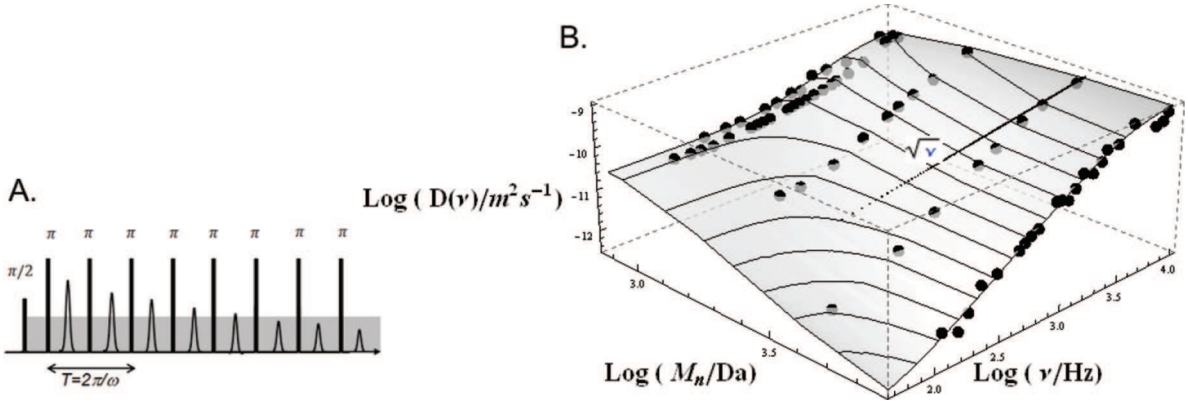

Fig. 1: (Colour on-line) (A) MGSE sequence used in experiment, where a train of π-RF pulses (black) is applied at a constant magnetic gradient (gray). (B) Velocity autocorrelation spectra, $D(\omega)$, of mono-disperse poly(isoprene-1.4) with different molecular mass plotted on the fitting surface given by eq. (8). The straight line indicates the spectra approach to the $\sqrt{\nu}$-dependence at high frequencies.

could be 50 kHz in the current state-of-the-art NMR devices. With π-RF pulses repeated in intervals $T/2$, shown in fig. 1(A), the spin-echo attenuation at the time of signal acquisition after n-th periods at $\tau = nT$, is

$$\beta(\tau, \omega_m) = \frac{8\gamma^2 G^2 \tau}{\pi^2 \omega_m^2} D(\omega_m); \quad \omega_m = \frac{2\pi}{T}. \tag{3}$$

The MGSE excels among other methods for studying molecular dynamics by its instant insight into different modes of molecular translational motion. Current applications of the method on various systems [45,46] have demonstrated its ability to provide an insight into the frequency range of molecular dynamics that so far has not been accessible by other experimental techniques. The advantage of the MGSE method with the constant gradient is also its ability to evaluate and thus to eliminate the effect of internal susceptibility fields, such as those in the polymer melt, by the variation of the applied gradient.

Molecular dynamics of a polymer melt. – Theoretical models commonly describe the molecular dynamics with the time-dependent mean squared displacement (MSD) $\langle \Delta z^2(t) \rangle$, which is related to $D(\omega)$ by the Fourier transformation $D(\omega) = -\frac{\omega^2}{2} FT \left[\langle \Delta z^2(t) \rangle \right]$. In the Rouse model [1], Brownian motion of beads connected by harmonic springs is presented as the diffusion of a single polymer chain. In the case of a long chain, averaging over all segments gives the segmental MSD as a sum of modes [9]

$$\langle \Delta z^2(t, N) \rangle_R = 2D_c t + 2D_s \tau_R \sum_{p=1}^{N} \frac{1}{p^2} (1 - \mathrm{e}^{-p^2 t/\tau_R}). \tag{4}$$

Here, $D_c = \frac{k_B T}{N\xi}$ is the center-of-mass diffusion coefficient of a coil with N Kuhn segments and where ξ is the effective friction drag coefficient on the monomer. $\tau_R = \frac{2\langle X_1^2 \rangle}{3D_c}$ is the Rouse relaxation time and $\langle X_1^2 \rangle$ is the amplitude of the Rouse mode. The segmental diffusion rate D_s is equal to D_c [9]. The Fourier transformation of MSD gives the segmental VAS

$$D(\omega, N)_R = D_c + D_s \sum_{p=1}^{N} \frac{p^2 \omega^2 \tau_R^2}{p^4 + \omega^2 \tau_R^2}. \tag{5}$$

In a polymer melt, intermolecular entanglements localize a macromolecule inside a curved tube. In short time intervals, the chain part between the adjacent entanglements, with lengths of a and with N_e Kuhn steps, moves as anticipated in the Rouse model with MSD $\langle \Delta z^2(t, N_e) \rangle_R$. In the intermediate time regime, as the segments reach the tube walls, the chain starts to reptate in the curvilinear manner along the tube with MSD $\langle \Delta z^2 \rangle_{rept} \propto d\sqrt{\langle \Delta z^2(t, N) \rangle_R}$, where d is the effective tube diameter. Correlations with the initial conformation are lost at longer times, when the polymer chain creeps out of the tube at the terminal time $\tau_d = \frac{N^2 a^2}{\pi^2 N_e^2 D_c} \propto N^3$ and MSD of the polymer is $\langle \Delta z^2 \rangle_d = 2D_d t$, where D_d is the self-diffusion coefficient of the center of mass in the polymer melt [2]. The substitution of the Rouse MSD in eq. (4) into the above expressions gives an overall MSD time dependence, which is proportional to $t^{1/2}$ at short times. In the intermediate regime of tube/reptation, MSD changes from $t^{1/4}$ to $t^{1/2}$ proportionality and, after the chain disengagement from the tube, to t as shown in fig. 5.

With the use of Fourier transformation of the segmental MSD in different time regimes, we obtain the overall diffusion spectrum $D(\omega)$ of entangled polymers, as shown in refs. [32,45]. With increasing frequency, $D(\omega)$ changes from the constant value, D_d, in the regime of disengagement, into the $\omega^{1/2}$-dependence at the transition into the regime of reptation at $\omega_d = 2\pi/\tau_d$. The reptation $D(\omega)$ passes at higher frequencies into the $\omega^{3/4}$-dependence, and then, after the transition in the regime of the Rouse chain motion at $\omega_R = 2\pi/\tau_R$, into the $\omega^{1/2}$-dependence. At very high frequencies, $D(\omega)$ levels to the constant value.

The tube/reptation model replaces the many-chain problem by a single chain moving in a tube of permanent obstacles, which are topological constraints exerted

by the surrounding chains. This model enables a solution, but is oversimplified due to the neglect of moving obstacles, which are responsible for the constraint release and relaxation of the tube [11,47]. The constraint release was originally termed as a tube reorganization by Pierre-Gilles de Gennes, in which the obstacle lifetime, τ_{ob}, determines the tube relaxation times [2]. Various models account for the impermanence of entanglements [48–50], among which the theory of constraint release involving tube dilation and tube-Rouse motion proposed by Viovy *et al.* [51]. In this approximation, the constrain release is considered as the tube-Rouse motion, in which a is the size of the segment, $\frac{N}{N_e}$ is the number of segments, $L_{eq} = \frac{N}{N_e}a$ is the curvilinear length of the tube chain, and the relaxation time is proportional to the lifetime of the obstacles $\tau_{ob}\frac{N^2}{N_e^2}$ [51]. The model of the tube-Rouse motion gives MSD of the tube as $\langle \Delta z^2 \rangle_{Rtube} = \langle \Delta z^2(t, N/N_e) \rangle_R$, which is derived from eq. (5) by the substitutions: $D_c \to D_d = \frac{N_e}{N} D_c$, $\langle X_1^2 \rangle \to \langle X_1^2 \rangle_{Rtube} = \frac{3L_{eq}a}{2\pi^2}$, $\tau_R \to \tau_{tR} = \tau_{ob}\frac{N^2}{N_e^2}$ and $D_s \to D_{st} = \frac{2\langle X_1^2 \rangle_{Rtube}}{3\tau_{tR}}$. According to this model, the chain relaxation in polymer melts is assumed to be a result of two independent and concurrent processes; the reptation inside the tube and the tube-Rouse motion as the tube reorganization. At low frequencies, the VAS of both processes starts from a constant D_d and changes to the $\sqrt{\omega}$-dependence at the terminal time, which is the longest relaxation time in the case of both models. In the case of mono-dispersed polymer melt, the tube reorganization is slower than reptation and must have a small effect on the diffusion properties [48,49], although, Graessley [47] showed that the tube reorganization significantly affects viscoelastic properties, presumably because of the difference between the spectrum of the tube-Rouse modes and the spectrum of reptation dynamics. For this reason, the kHz-frequency range of the MGSE method is particularly suitable to examine the range of transition from the chain reptation to the chain disengagement, in which the spectrum is supposed to change from the constant D_d into the $\omega^{1/2}$-dependence [32,45]. The method may provide a deeper insight into the effects of tube constraint release and clarify the interplay between the chain reptation in the tube and the tube reorganization.

Measurement. – The experiments were performed in the stray magnetic field of a single-side NMR-MOUSE device with a proton Larmor frequency of 11.7 MHz and a constant magnetic field gradient $G = 11.5\,\mathrm{T/m}$ using the Carr-Purcell-Meiboom-Gill (CPMG) train of 2.8 μs long π-RF pulses as shown in fig. 1(A). Our set-up permits the RF-pulse interval in the range from 50 μs to 10 ms, limiting the MGSE measurement of spectra to the frequency interval between 50 Hz and 10 kHz. An additional low-frequency limiting factor could be the signal attenuation at long time intervals between RF pulses, because the magnetic field gradient cannot be changed. We studied the segmental motion in mono-disperse poly(isoprene-1.4) (Polymer Standards Service GmbH, Mainz) at a temperature of 26 °C. Figure 1(B) shows the result of measurements on the polymer samples with different number average molecular masses: the samples with $M_n = 704\,\mathrm{Da}$ and $M_n = 835\,\mathrm{Da}$ with $M_w/M_n = 1.17$, the samples with $M_n = 1610\,\mathrm{Da}$ and $M_n = 3620\,\mathrm{Da}$ with $M_w/M_n = 1.05$ as well as the sample with $M_n = 7570\,\mathrm{Da}$ with $M_w/M_n = 1.05$, where the ratio of the mass average to the number average of molecular mass, M_w/M_n, determines the dispersivity of the polymer melt.

Discussion. – The obtained $D(\omega)$ spectra do not exhibit the anticipated transition from a constant value D_d into the $\sqrt{\omega}$-dependence although they show a weak indication to this approach at highest frequencies available by our set-up as shown in fig. 1(B). However, these spectra reflect the segmental diffusion in polymer melt, which was already observed by steady or pulsed GSE [14,25] termed as the anomalous diffusion. The MGSE method applied on the NMR mouse permits measurements up to 10 kHz, which means that in the time domain the measurement in the intervals, $T/2$, goes down to 50 μs. This allows a more detailed insight into the nature of anomalous diffusion by observing the segmental displacements in the intervals, which are more than two orders of magnitude smaller than by ordinary pulsed or steady GSE. The time dependence of the self-diffusion coefficient, which is correctly derived from Einstein's relation as

$$D(\tau) = \frac{1}{2}\frac{\mathrm{d}\langle \Delta x^2 \rangle}{\mathrm{d}\tau} = \frac{2}{\pi}\int_0^\infty D(\omega)\frac{\sin(\tau\omega)}{\omega}\mathrm{d}\omega, \qquad (6)$$

differs from the time dependence of the apparent diffusion coefficient given, either from pulsed GSE shown in ref. [32], or from steady GSE, as

$$\ln S(\tau)/S_0 = \frac{1}{\pi}\int_0^\infty D(\omega)\frac{\sin^4(\tau\omega/4)}{\omega^4}\mathrm{d}\omega = q^2 D_{app}(\tau)\tau, \quad (7)$$

where $q^2 = \gamma^2 G^2 \tau^2/12$. This digression may explain the fact that the values evaluated from the NMR diffusometry turned out to be much too large with respect to that of models [27] and therefore the results of MGSE and GSE measurements are incomparable.

Our analysis of the MGSE data, quite unexpectedly, provides an empiric formula similar to that of the Rouse spectrum, which fits almost perfectly to the experimental data presented in fig. 1(B). In the literature, we found an explanation in ref. [51], if considering the empiric formula as the first term of the spectrum for the tube-Rouse motion given in eq. (5)

$$D(\omega, N)_{tR} = D_d + D_{st}\frac{\omega^2\tau_{tR}^2}{1+\omega^2\tau_{tR}^2}. \qquad (8)$$

An excellent fit leads us to the interpretation of the tube-Rouse motion as a dominant process of polymer dynamics in the time interval close to the chain disengagement. The

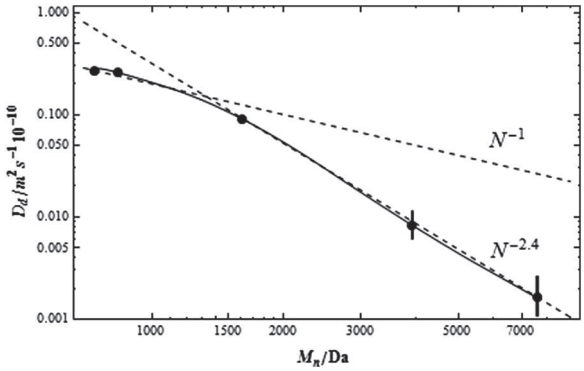

Fig. 2: The dependence of the polymer center-of-mass diffusion coefficient on the molecular mass from the fit of eq. (8) to the experimental data. Missing error bars indicate fitting errors smaller than the width of the plot-marker.

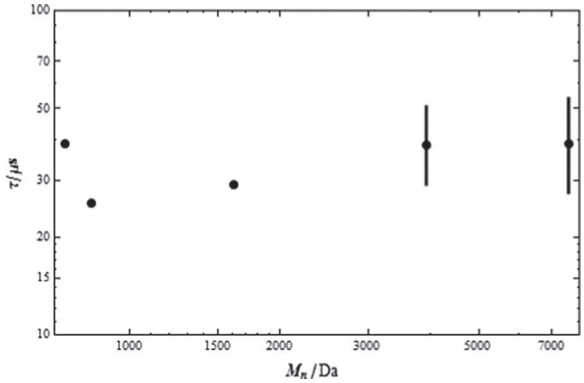

Fig. 3: Relaxation time of the tube-Rouse motion as a function of the molecular mass from the fit of eq. (8) to the experimental data. Missing error bars indicate fitting errors smaller than the width of the plot-marker.

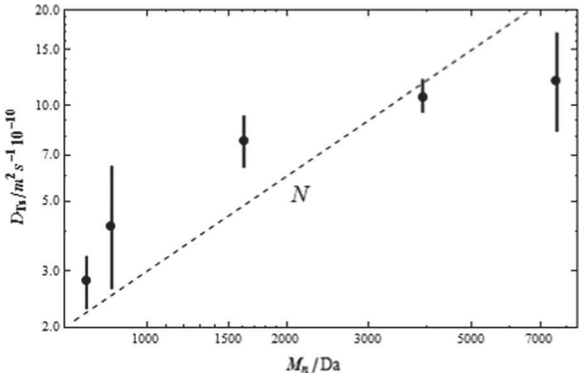

Fig. 4: Tube segmental diffusion rate, D_{ts}, obtained from the fit of eq. (8) to the experimental data.

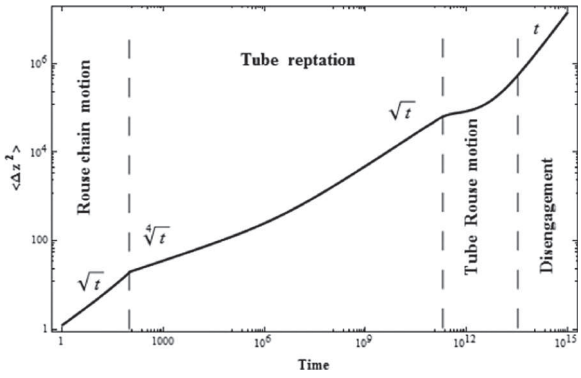

Fig. 5: The time dependence of the MSD in different regimes of polymer motion with the addition of the tube-Rouse motion regime as derived from the Fourier transformation of $D(\omega)$ shown in fig. 1.

extrapolations of fitting curves to low frequencies, beyond the reach of the method, provide the values that could be the center-of-mass diffusion coefficients, D_d. Its molecular mass dependence displays a pronounced transition from the N^{-1} into the $N^{-2.4}$-scaling around the molecular mass $M_n = 1000$–$1700\,\mathrm{Da}$ as shown in fig. 2. The poly(isoprene-1.4) macromolecule consists of monomers with a relative molecular mass of 68 Da, and with 4.6 monomers per Kuhn step [52]. This implicates the transition into a regime of entanglement in the range of $N \approx 3$–5, which is less than predicted by theories [4–7] and simulations [8–10]. The error bars shown in the figures are parameter variations of the least squared fit to the experimental data with the assumption of error normal distributions. Figure 3 shows the relaxation times, which are almost independent of the molecular mass, although the theory predicts N^5-dependence in the case of the tube-Rouse motion in the mono-dispersed polymer melt [51]. This result could indicate that the tube rearrangement relaxation processes are not determined solely by the disengagement time of surrounding chains. Figure 4 shows also that the diffusion rate of tube segments, denoted as D_{st} in eq. (8), does not follow exactly the predicted linear dependence on N [51], which could mean that the interpretation with the tube-Rouse motion is questionable. Brownian particles coupled to attractive centers exhibit a similar decline of VAS at low frequencies, offering an alternative interpretation of experimental data. A new model may also explain the increase of $D(\omega)$ with molecular mass at high frequencies as shown in fig. 1(B).

Conclusions. – The measurement of the velocity autocorrelation spectrum of molten polymers with the MGSE method provides new information on polymer dynamics, for which no clear explanation is yet known. A good agreement between the measured spectra and the spectrum given by the Rouse model leads to an interpretation which is closer to the model of tube-Rouse motion as the dominant process in the range of polymer chain disengagement from the tube. With the conversion of the frequency spectrum to the time domain, a new intermediate MSD time dependence can be identified between the chain reptation and the chain disengagement as shown in fig. 5. We expect that these results could potentially help to develop more accurate models of polymer dynamics and provide a better

explanation of the tube "constraint release". A new theory may also clarify unusual low-frequency spectra similar to those of the polymers, which were found in liquids with the strong hydrogen bonding by the MGSE method [45].

* * *

We are grateful to the Slovenian Ministry of Higher Education, Science and Technology for the financial support.

REFERENCES

[1] Rouse P., *J. Chem. Phys.*, **21** (1953) 1272.
[2] de Gennes P., *J. Chem. Phys.*, **55** (1971) 572.
[3] Doi M. and Edwards S. F., *J. Chem. Soc., Faraday Trans.*, **74** (1978) 1789.
[4] Rubinstein M., *Phys. Rev. Lett.*, **59** (1987) 1946.
[5] des Cloizeaux J., *Europhys. Lett.*, **5** (1988) 437.
[6] Schweizer K., *J. Chem. Phys.*, **91** (1989) 5822.
[7] Guenza M., *J. Chem. Phys.*, **110** (1999) 7574.
[8] Harmandaris V. A., Mavrantzas V. G., Theodorou D. N., Kroeger M., Ramirez J., Oettinger H. C. and Vlassopoulos D., *Macromolecules*, **36** (2003) 1376.
[9] Perez-Aparicio R., Colmenero J., Alvarez F., Padding J. T. and Briels W. J., *J. Chem. Phys.*, **132** (2010) 0249045.
[10] Bulacua M. and van der Giessen E., *J. Chem. Phys*, **123** (2005) 114901.
[11] McLeish T. C. B., *Adv. Phys.*, **51** (2002) 1379.
[12] Ewen B. and Richter D., *Adv. Polym. Sci.*, **134** (1997) 1.
[13] Stapf S. and Kimmichh R., *Macromolecules*, **29** (1996) 1638.
[14] Kimmich R. and Fatkullin N., *Adv. Polym. Sci.*, **170** (2004) 1.
[15] Graf R., Heuer A. and Spiess H. W., *Phys. Rev. E*, **52** (1998) 3273.
[16] Cháves F. V. and Saalwächter K., *Phys. Rev. Lett*, **104** (2010) 198305.
[17] Komlosh M. E. and Callaghan P. T., *J. Chem. Phys.*, **109** (1998) 10053.
[18] Cohen-Addad J. P., *J. Phys. (Paris)*, **43** (1982) 1509.
[19] Fatkullin N., Mattea C. and Stapf S., *J. Chem. Phys.*, **139** (2013) 194905.
[20] Herrmann A., Kresse B., Wohlfahrt M., Bauer I., Privalov A. F., Kruk D., Fatkullin N., Fujar F. and Rössler E. A., *Macromolecules*, **45** (2012) 6516.
[21] Kruk D., Herrmann A. and Rössler E., *Prog. Nucl. Magn. Reson. Spectrosc.*, **63** (2012) 33.
[22] Meier R., Herrmann A., Hofmann M., Schmidtke B., Kresse B., Privalov A. F., Kruk D., Fujara F. and Rössler E. A., *Macromolecules*, **46** (2013) 5538.
[23] Saalwächter K., *Prog. Nucl. Magn. Reson. Spectrosc.*, **51** (2007) 1.
[24] Fleischer G., *Colloid Polym. Sci.*, **265** (1987) 89.
[25] Appel M., Fleischer G., Kaerger J., Fujara F. and Chang I., *Macromolecules*, **27** (1994) 4274.
[26] Fatkullin N. and Kimmich R., *Phys. Rev. Lett.*, **802** (1995) 5738.
[27] Fischer E., Kimmich R., Fatkullin N. and Yatsenko G., *Phys. Rev. E*, **62** (2000) 775.
[28] von Meerwall E., Ozisik R., Mattice W. L. and Pfister P. M., *J. Chem. Phys.*, **118** (2003) 3867.
[29] von Meerwall E. D., Dirama N. and Mattice W. L., *Macromolecules*, **40** (2007) 3970.
[30] Bar-Shir A., Avram L., Ozarslan E., Basser P. and Cohen Y., *J. Magn. Reson.*, **194** (2008) 230.
[31] Price W. S., *Concepts Magn. Reson.*, **10** (1998) 197.
[32] Stepišnik J., Lahajnar G., Zupančič I. and Mohorič A., *J. Magn. Reson.*, **236** (2013) 41.
[33] Callaghan P. and Stepišnik J., *J. Magn. Reson. A*, **117** (1995) 118.
[34] Stepišnik J., *Physica B*, **104** (1981) 350.
[35] Stepišnik J., *Prog. Nucl. Magn. Reson. Spectrosc.*, **17** (1985) 187.
[36] Callaghan P. and Stepišnik J., *Advances in Magnetic and Optical Resonance*, edited by Warren Warren S., Vol. **19** (Academic Press, Inc, San Diego) 1996, Chapt. "Generalised Analysis of Motion Using Magnetic Field Gradients", pp. 326–389.
[37] Stepišnik J. and Callaghan P., *Physica B*, **292** (2000) 296.
[38] Callaghan P. T. and Codd S. L., *Phys. Fluids*, **13** (2001) 421.
[39] Topgaard D., Malmborg C. and Soederman O., *J. Magn. Reson.*, **156** (2002) 195.
[40] Parsons E. C., Does M. D. and Gore J. C., *Magn. Reson. Imaging*, **21** (2003) 279.
[41] Meiboom S. and Gill D., *Rev. Sci. Instrum.*, **29** (1958) 688.
[42] Lasič S., Stepišnik J., Mohorič A., Serša I. and Planinšič G., *Europhys. Lett.*, **75** (2006) 887.
[43] Lasič S., Stepišnik J. and Mohorič A., *J. Magn. Reson.*, **182** (2006) 208.
[44] Stepišnik J., Lasič S., Mohoricč A., Serša I. and Sepe A., *J. Magn. Reson.*, **182** (2006) 195.
[45] Stepišnik J., Mohorič A., Serša I. and Lahajnar G., *Macromol. Symp.*, **305** (2011) 55.
[46] Stepišnik J., Fritzinger B., Scheler U. and Mohoriič A., *EPL*, **98** (2012) 57009.
[47] Graessley W., *Adv. Polym. Sci.*, **47** (1982) 67.
[48] Klein J., *J. Macromol.*, **11** (1978) 825.
[49] Daoud M. and de Gennes P. G., *J. Polym. Sci: Polym. Phys. Ed.*, **17** (1979) 1971.
[50] Leygue A., Bailly C. and Keunings R., *J. Chem. Phys.*, **128** (2005) 23.
[51] Viovy J., Rubinstein M. and Colby R., *Macromolecules*, **24** (1991) 3587.
[52] Fetters L. J., Lohse D. J. and Colby R. H., *Physical Properties of Polymers Handbook*, Vol. **2** (AIP Press, Woodbury, New York) 2006, Chapt. "Chain Dimensions and Entanglement Spacings", pp. 445–452.